# Single Cell Matrix-Assisted Laser Desorption/Ionization Mass Spectrometry Imaging

**ARTICLE** *in* ANALYTICAL CHEMISTRY · JULY 2012

Impact Factor: 5.64 · DOI: 10.1021/ac301337h · Source: PubMed



**4 AUTHORS**, INCLUDING:

Yvonne Schober
Philipps University of Marburg
**13** PUBLICATIONS **253** CITATIONS
SEE PROFILE

Sabine Schulz
Justus-Liebig-Universität Gießen
**17** PUBLICATIONS **541** CITATIONS
SEE PROFILE

analytical chemistry

Letter

pubs.acs.org/ac

# Single Cell Matrix-Assisted Laser Desorption/Ionization Mass Spectrometry Imaging

Yvonne Schober, Sabine Guenther, Bernhard Spengler, and Andreas Römpp*

Institute of Inorganic and Analytical Chemistry, Justus Liebig University, Giessen, Germany

Supporting Information

**ABSTRACT:** Application of mass spectrometry imaging (MS imaging) analysis to single cells was so far restricted either by spatial resolution in the case of matrix-assisted laser desorption/ionization (MALDI) or by mass resolution/mass range in the case of secondary ion mass spectrometry (SIMS). In this study we demonstrate for the first time the combination of high spatial resolution (7 $\mu$m pixel), high mass accuracy (<3 ppm rms), and high mass resolution ($R$ = 100 000 at $m/z$ = 200) in the same MS imaging measurement of single cells. HeLa cells were grown directly on indium tin oxide (ITO) coated glass slides. A dedicated sample preparation protocol was developed including fixation with glutaraldehyde and matrix coating with a pneumatic spraying device. Mass spectrometry imaging measurements with 7 $\mu$m pixel size were performed with a high resolution atmospheric-pressure matrix-assisted laser desorption/ionization (AP-MALDI) imaging source attached to an Exactive Orbitrap mass spectrometer. Selected ion images were generated with a bin width of $\Delta m/z$ = ±0.005. Selected ion images and optical fluorescence images of HeLa cells showed excellent correlation. Examples demonstrate that a lower mass resolution and a lower spatial resolution would result in a significant loss of information. High mass accuracy measurements of better than 3 ppm (root-mean-square) under imaging conditions provide confident identification of imaged compounds. Numerous compounds including small metabolites such as adenine, guanine, and cholesterol as well as different lipid classes such as phosphatidylcholine, sphingomyelin, diglycerides, and triglycerides were detected and identified based on a mass spectrum acquired from an individual spot of 7 $\mu$m in diameter. These measurements provide molecularly specific images of larger metabolites (phospholipids) in native single cells. The developed method can be used for a wide range of detailed investigations of metabolic changes in single cells.

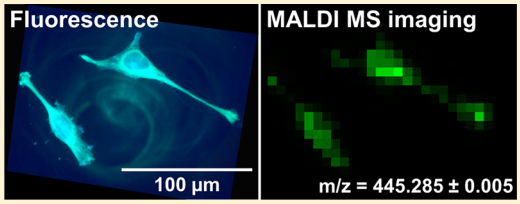


Mass spectrometry imaging (MS imaging) has become a widely used analytical technique due to its ability to visualize the distribution of a large variety of analytes.[1−5] Numerous applications have been published including the imaging of lipids,[6] peptides,[7,8] and proteins.[9] The spatial resolution has been significantly increased in recent years. However, the analysis of larger biomolecules/metabolic profiles in single cells remains a challenging task.

Cell cultures are model systems that are used to investigate disease-related and physiological processes. The influence of pathogenic or environmental factors can be studied under controlled conditions in cell cultures. Metabolic studies are usually based on the analysis of bulk samples. The analysis of individual cells would instead provide much more specific and informative data. A summary on this topic was recently published by Svatos.[10] The author concluded that several techniques can provide metabolic information from single cells, but each method still has significant limitations. Commonly used techniques such as optical and staining methods led to important discoveries but often lack molecular specificity. Mass spectrometry-based methods on the other hand face a number of practical and experimental problems.

Time-of-flight secondary ion mass spectrometry (TOF-SIMS) offers submicrometer spatial resolution and is thus able to image the spatial distribution of metabolites inside single cells.[11,12] A recent review on SIMS can be found in ref 13. However, TOF-SIMS for single cell analysis is typically limited in mass range to $m/z$ < 500, and detected analytes can often not be identified.[14] This is due to severe fragmentation of larger analyte ions and limited tandem mass spectrometry (MS/MS) capabilities in the imaging mode. Fragmentation can be reduced by modifications such as matrix-enhanced (ME)-SIMS, which was used for the analysis of lipids in single cells.[15] The authors of this study also implemented metal-assisted (MetA) SIMS which lead to the detection of signals up to $m/z$ = 1000. MS/MS experiments in single cell imaging were reported for cholesterol.[16] High resolution mass analyzers ($R$ > 10 000) for SIMS have been developed[16,17] but are so far not available for imaging at cellular resolution.

Mass spectrometry imaging methods based on matrix assisted laser desorption/ionization (MALDI), on the other hand, offer a higher mass range (and mass resolution). Pixel size, however, is typically in the range of 50−200 $\mu$m, and thus single cell structures cannot be resolved with established approaches. Direct analysis of single cells with these methods results in only one pixel per cell at a pixel size of 50 $\mu$m.[18] An alternative is to use stretched media in order to expand the

**Received:** May 16, 2012
**Accepted:** July 17, 2012
**Published:** July 17, 2012

   dx.doi.org/10.1021/ac301337h | *Anal. Chem.* 2012, 84, 6293−6297

original spatial structure.[19] Application of this method to single cells was demonstrated, resulting in a spatial resolution of about 40 $\mu$m.[20] Peptides were identified, but intracellular spatial information was very limited. This indirect approach is also challenging in terms of alignment of data and correlation with alternative (optical) techniques. Another method is laser desorption ionization (LDI) which was used for the analysis of single cells within plant tissue.[21] This approach does not require any matrix application but is limited to compounds with UV-absorbing functional groups.

A critical step in single cell analysis is sample preparation. It has to be compatible with experimental conditions, i.e., with high vacuum in SIMS[22] and with matrix coating in MALDI, respectively. This treatment can put considerable strain on the spatial integrity of biological samples in general and single cells in particular. Cells may burst, which usually increases signal intensity due to leaking of cell components on the sample support, but obviously all spatial information is lost.

The quality of the MS images does not only depend on spatial resolution but also on specificity and reliability of mass spectral data. Reliability of compound identification can be significantly increased by accurate mass measurements. Mass spectrometers with mass accuracies in the low ppm range are routinely used in many bioanalytical areas, but only few applications were reported for MS imaging. High resolution mass spectra are especially useful to resolve the complexity of biological samples in MS imaging as these experiments do not include any separation step (e.g., chromatography) before MS analysis. We recently introduced a mass spectrometry imaging method that combines high resolution/accurate mass measurements on tissue with spatial resolution in the low micrometer range and MS/MS capability for the analysis of lipids,[23] drug compounds,[24] and neuropeptides.[25]

In the current study we developed a dedicated sample preparation protocol for single cells analysis and applied our high resolution mass spectrometry imaging method. These measurements provide molecularly specific image analysis of larger metabolites (phospholipids) in native single cells. Molecular identification and specificity were provided by high quality mass spectral data.

## EXPERIMENTAL SECTION

**Sample Preparation.** HeLa cells, an immortalized human cell line derived from cervical cancer, were directly grown on indium tin oxide (ITO) coated glass slides in serum free media (Quantum 101 for HeLa cells with L-Glutamine, PAA, Pasching Austria) for 12 h in an incubator at 37 °C and an atmosphere of 5% $CO_2$. After aspiration of media, the cells were washed two times with phosphate buffered saline (PBS) (Dulbeccoś PBS, PAA, Pasching, Austria) followed by fixation in 0.25% glutaraldehyde (EM grade, Agar Scientific, Essex, Great Britain) for 15 min. This fixation step leads to cross-linking of proteins in the cells. Buffer solutions were kept at 37 °C in order to prevent disruption of cells before fixation. Afterward the cells were stained with 3,3′-dihexyloxacarbocyanine iodide ($DIOC_6(3)$) (Invitrogen Live Technologies GmbH, Darmstadt, Germany) ($c$ = 0.001 $\mu$g/mL) in PBS for 5 min. $DIOC_6(3)$ is a fluorescence dye which stains cell membranes.[26] The final step was rinsing the cells with pure water (room temperature) in order to remove excessive $DIOC_6(3)$ from the sample. Fluorescence images of the sample were acquired with an Olympus BX-40 microscope (Olympus Europa GmbH, Hamburg, Germany) at an emission wavelength of 501 nm prior to matrix application. The sample was covered with matrix by applying 150 $\mu$L of 2,5-dihydroxybenzoic acid (DHB) solution (30 mg/mL in 50:50 acetone/water/0.5% TFA) with a home-built pneumatic sprayer.[27] Details on necessary safety precautions can be found in the Supporting Information.

**MALDI MS Imaging.** All experiments were performed using an atmospheric-pressure matrix-assisted laser desorption/ionization (AP-MALDI) high resolution imaging source (TransMIT GmbH, Giessen, Germany) attached to a Fourier transform orbital trapping mass spectrometer (Exactive Orbitrap, Thermo Fisher Scientific GmbH, Bremen, Germany). The ion optical and laser setup[28,29] as well as details on the measurement procedure[23] are described elsewhere. The step size of the sample stage was set to 7 $\mu$m. The ablation area caused by the laser was about 5 $\mu$m in diameter (see the Supporting Information Figure S-1 for details). A total of 30 laser pulses were summed for each mass spectrum. Mass spectrometric measurements were performed in positive-ion mode in the mass to charge range $m/z$ = 100−1000. Mass resolution was set to $R$ = 100 000 at $m/z$ = 200. Mass spectra were internally calibrated using the lock mass feature of the instrument. Selected ion images were generated using the software package MIRION developed in-house. This software can read "raw" data files generated by the Exactive Tune software (Thermo Fisher Scientific GmbH, Bremen, Germany) and link the mass spectra to spatial information provided in a separate file. More details on this procedure can be found in ref 28. Selected ion images were created with a bin width of $\Delta m/z$ = ±0.005. Intensity values in ion images were normalized to the highest intensity measured for each ion species separately. No other postprocessing steps such as interpolation or normalization to matrix signals were applied to the images, in order to demonstrate the original data quality.

## RESULTS AND DISCUSSION

Sample preparation is a critical step in obtaining useful results in mass spectrometry imaging, especially at high spatial resolution. Fixation methods with ethanol or formaldehyde turned out to be not suited for the adhesive cells on ITO-

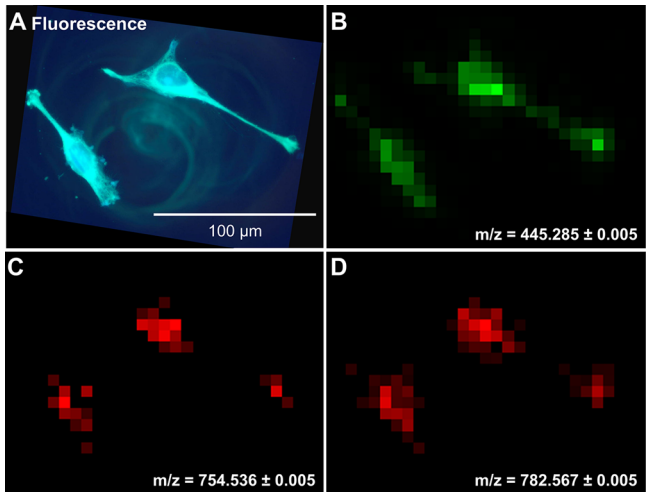


**Figure 1.** HeLa cells on ITO slide (A) optical fluorescence of $DIOC_6(3)$ stained HeLa cells, $\lambda$ = 501 nm. (B−D) MALDI imaging (28 × 21 pixels, pixel size 7 $\mu$m): (B) selected ion image of staining agent $DIOC_6(3)$ ($[M]^+$), (C) selected ion image of PC(32:1) ($[M + Na]^+$), and (D) selected ion image of PC(34:1) ($[M + Na]^+$).


dx.doi.org/10.1021/ac301337h | Anal. Chem. 2012, 84, 6293−6297

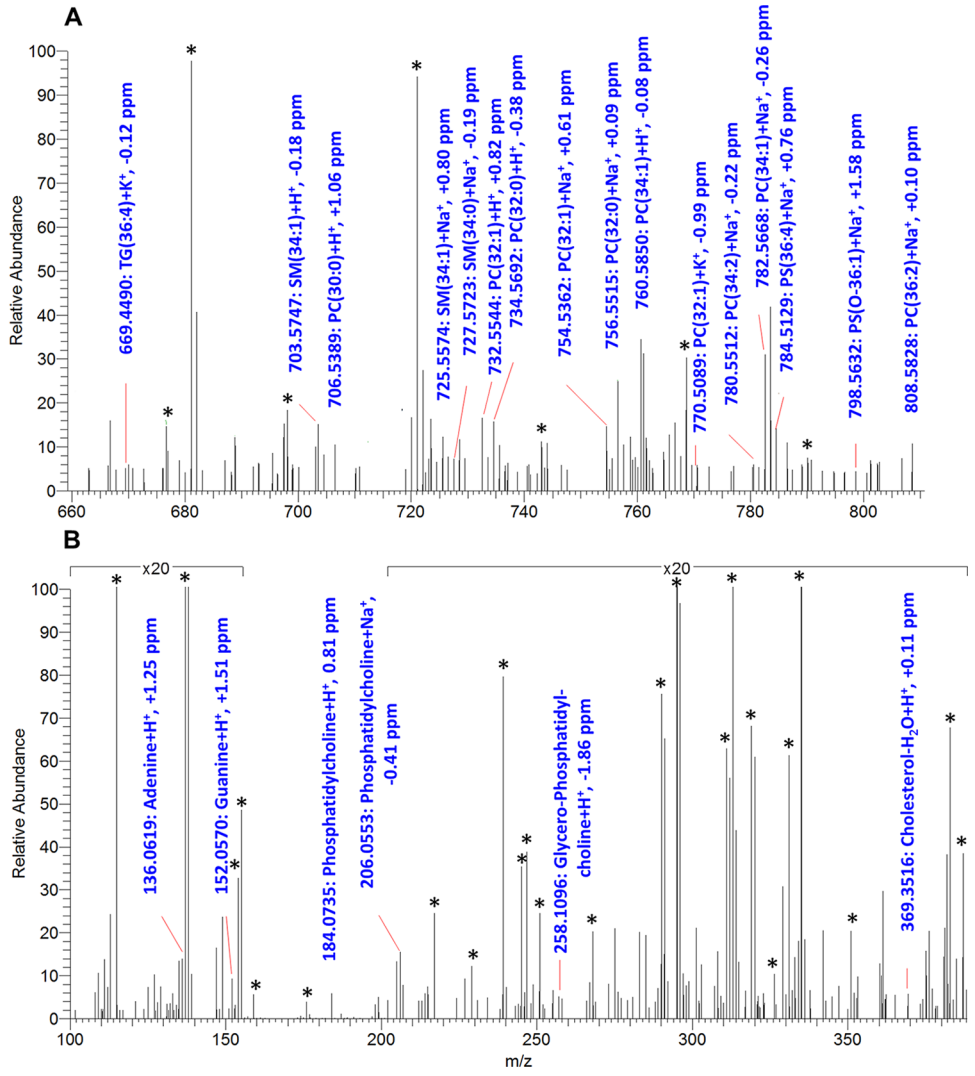


**Figure 2.** Mass spectrum acquired from a single 7 $\mu$m pixel for mass range $m/z$ = 620−810 (A) and $m/z$ = 100-380. (B) Identified compounds are labeled with measured mass, compound name, and mass deviation. See Table S-1 in the Supporting Information for more details. Background peaks (e.g., from matrix or sample support) are marked with an asterisk.

coated glass slides used in this study. This treatment resulted in loss of the cells during the sample preparation procedure.

Fixation of cells with glutaraldehyde delivered the best results for analysis with MALDI MS imaging. Experimental details such as temperature of solutions, buffer concentration, and incubation times turned out to be critical and were carefully optimized (see the Experimental Section for details). The final washing step (after $DIOC_6(3)$ staining) was necessary because unbound staining agent results in high background signal in mass spectra (due to its cationic nature). To remove excessive $DIOC_6(3)$ we used pure water instead of a buffer solution in order to avoid crystallization on the sample which would interfere with the MS measurement. Cells were grown directly on the substrate for MS imaging (ITO-coated glass slides), which allows one to investigate the native structure of these adhesive cells. Staining with $DIOC_6(3)$ was found to be compatible with MS imaging analysis and delivered optical fluorescence images for direct comparison. After matrix deposition an area of 749 × 749 $\mu m^2$ was measured with a pixel size of 7 $\mu$m (107 × 107 pixels). Mass spectra were acquired for a mass range of $m/z$ = 100−1000. A detail of the measured area (28 × 18 pixels, 196 × 126 $\mu m^2$) including two individual HeLa cells is shown in Figure 1. The signal of $DIOC_6(3)$ in optical fluorescence mode (wavelength $\lambda$ = 501 nm) and the MS imaging experiment (selected ion image of $m/z$ = 445.285 ± 0.005) are shown in parts A and B of Figure 1, respectively. The two measurements show excellent correlation. The integrity of the cells was apparently preserved throughout the whole workflow of this experiment (i.e., the cells did not burst). This is an essential prerequisite in order to obtain useful spatial information of these biological samples. The shape of the cells is clearly visible in the MS image and even small extensions of only a few micrometers in diameter were still detectable. This implies that the spatial features of the cells were not significantly affected by the matrix application and the measurement procedure. These MS images also demonstrate that features in the range of a few micrometers can be detected with our method. Figure 1C,D shows the selected ion images of two phospholipids. The sodium adduct signal of phosphatidylcholine PC(32:1) and PC(34:1) were detected primarily in the center of the cell, where higher concentrations of membranes are expected.[30] This is in agreement with the distribution of the lipophilic staining agent $DIOC_6(3)$ (Figure 1A) which selectively stains membranes.[26,31]


dx.doi.org/10.1021/ac301337h | *Anal. Chem.* 2012, 84, 6293−6297

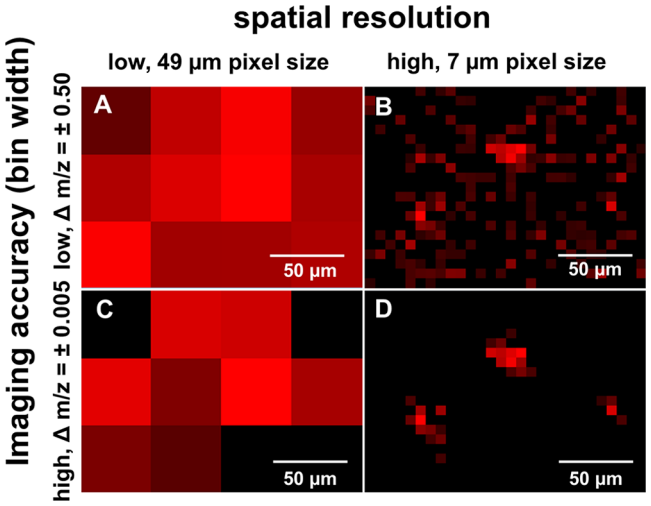


**Figure 3.** Influence of imaging accuracy (bin width) and spatial resolution on the information contents of selected ion images shown for the example of $m/z$ = 754.536 (sodium adduct of PC (32:1)); see Figure 1A for the corresponding fluorescence image. (A–C) Selected ion images recalculated for acquisition parameters of previous studies. (D) Selected ion image obtained in this work based on high spatial resolution (7 $\mu$m) and high imaging accuracy ($m/z$ = 754.536 ± 0.005); this image is identical with Figure 1C.

As noted above, Figure 1 only shows a small part of the measurement. Optical and MS images of the entire measurement area and of two other zoomed-in areas are shown in the Supporting Information (Figures S-2 and S-3).

Apart from the two lipids shown in Figure 1, a set of other metabolites was detected in these measurements. Figure 2 shows a mass spectrum from a single 7 $\mu$m pixel. Numerous phospholipids such as phosphatidylcholine (PC), sphingomyeline (SM), phosphatidylserine (PS), as well as di- (DG) and trigylcerides (TG) were detected in the mass range $m/z$ = 620–810 (Figure 2A). A more detailed section ($m/z$ = 754–761) of an averaged mass spectrum is shown in Figure S-4a in the Supporting Information.

Detected compounds were identified using accurate mass values (<3 ppm) for database searches in LIPID MAPS[32] and Metlin.[33] The mass spectra contained a number of peaks which originate from the matrix or sample support (marked with an asterisk in Figure 2). A background spectrum acquired between cells is shown in Figure S-4b in the Supporting Information for comparison. The lipids shown in Figure 1 were investigated in more detail by additional MS/MS measurements of a more densely grown cell population (see the Supporting Information, Figure S-5). Analysis of the fragment ions allowed assignment of the individual acyl chains resulting in the identification of PC(16:0/16:1) and PC(16:0/18:1). In addition to phospholipids, smaller metabolites such as adenine, guanine, and cholesterol were detected in the mass range $m/z$ = 100–380 (Figure 2B). All compounds were detected with a mass accuracy of better than 3 ppm (rms) for the complete image, providing reliable substance identification. Mass resolving power ranged from 20 000 to 100 000 depending on the mass to charge ratio of the detected compounds. Detailed information on detected compounds including mass accuracy and mass resolution is provided in the Supporting Information (Table S-1). Consequently a full metabolic profile can be acquired from a defined area of the cell with high confidence. Alternatively several spectra from one cell can be combined in order to obtain better statistics for quantitative analysis. The cell material is completely consumed in the area ablated by the laser beam, i.e., the obtained mass spectra contain information about cell walls, cytoplasm, and nucleus (as evidenced by the detection of adenine and guanine).

The effect of improved spatial resolution and imaging accuracy of our method is illustrated in Figure 3. The original data as acquired in our study is shown in Figure 3D. The phospholipid signal from the two individual cells is clearly visible. Figure 3C shows a recalculated image at a pixel size of 49 $\mu$m, resembling the spatial resolution of published MALDI imaging experiments. As expected the cells are not distinguishable any more. High spatial resolution alone is not sufficient to resolve the structure of single cells. Figure 3B shows a recalculated image generated with unit resolution ($\Delta m/z$ = 1), resembling the imaging accuracy of typical TOF-SIMS measurements. Low imaging accuracy leads to overlap of neighboring mass peaks and loss of specificity, and thus spatial information on PC(32:1) is lost. All selected ion images in our study were generated with a bin width of $\Delta m/z$ = ±0.005. It can be derived from our study that highly specific and detailed images of single cells are only possible if a spatial resolution in the low micrometer range and a mass accuracy in the low ppm range are combined within one experiment.

Our method can be used for a detailed investigation of metabolic changes in single cells. Current experiments are focused on the phospholipid mass range. Invasion mechanisms of pathogens are known to lead to changes in the lipid pattern through enzymatic degradation.[34] These effects can be investigated with high molecular specificity in single cells at different stages of the infection process with the methodology described here. Measurements can be further optimized for other $m/z$ ranges and substance classes by adjusting experimental parameters such as ion optics and laser energy settings. The detection of peptides is most likely affected by the cross-linking with glutaraldehyde, but carbohydrates, nucleic acids, and lipid compounds are accessible. Although the presented method represents a significant improvement for MALDI imaging of single cells, TOF-SIMS experiments still offer better spatial resolution.[15] TOF-SIMS also offers the advantage of 3D imaging of cells,[22] which is currently not possible with our method. A combination of mass spectrometry imaging experiments using SIMS for ultimate spatial information and MALDI for confident identification and increased mass range would provide a very powerful tool for the analysis of single cells.

## ■ CONCLUSIONS

We developed a method which allows one to image and identify larger metabolites (including phospholipids) in intact single cells. A metabolic profile can be obtained from a single 7 $\mu$m pixel and thus of well-defined segments of cells. Previous mass spectrometry imaging methods provided either high spatial resolution (SIMS) or sufficient mass accuracy and mass range (MALDI) but not simultaneously. Optical methods on the other hand can visualize only specific compounds which have to be labeled in a targeted approach. Future experiments will include the investigation of the invasion process of pathogens in single cells. The number of identified compounds will be further increased by measurements in the negative ion mode and additional MS/MS experiments. Spatial resolution and sensitivity will be improved by further optimization of sample preparation and measurement parameters.


dx.doi.org/10.1021/ac301337h | *Anal. Chem.* 2012, 84, 6293–6297

## ■ ASSOCIATED CONTENT

### Supporting Information

Additional information as noted in text. This material is available free of charge via the Internet at http://pubs.acs.org.

## ■ AUTHOR INFORMATION


### Corresponding Author

*Address: Justus Liebig University Giessen, Institute of Inorganic and Analytical Chemistry, Schubertstrasse 60, Building 16, 35392 Giessen, Germany. Phone: +49 641 99 34802. Fax: +49 641 99 34809. E-mail: andreas.roempp@anorg.chemie.uni-giessen.de.


### Notes

The authors declare no competing financial interest.

## ■ ACKNOWLEDGMENTS

Financial support by the State of Hesse (LOEWE Research Focus "Ambiprobe") is gratefully acknowledged. This publication represents a component of the Doctoral (Dr. rer. nat.) Thesis of Y.S. at the Faculty of Biology and Chemistry, Justus Liebig University Giessen, Germany.

## ■ REFERENCES


(1) Chughtai, K.; Heeren, R. M. A. *Chem. Rev.* **2010**, *110*, 3237−3277.
(2) McDonnell, L. A.; Heeren, R. M. A. *Mass Spectrom. Rev.* **2007**, *26*, 606−643.
(3) Spengler, B.; Hubert, M. *J. Am. Soc. Mass Spectrom.* **2002**, *13*, 735−748.
(4) Spengler, B.; Hubert, M.; Kaufmann, R. *42nd ASMS Conference on Mass Spectrometry and Allied Topics*, Chicago, IL, May 29−June 3, 1994; p 1041.
(5) Stoeckli, M.; Chaurand, P.; Hallahan, D. E.; Caprioli, R. M. *Nat. Med.* **2001**, *7*, 493−496.
(6) Jackson, S. N.; Wang, H. Y. J.; Woods, A. S. *J. Am. Soc. Mass Spectrom.* **2005**, *16*, 2052−2056.
(7) Chen, R. B.; Jiang, X. Y.; Conaway, M. C. P.; Mohtashemi, I.; Hui, L. M.; Viner, R.; Li, L. J. *J. Proteome Res.* **2010**, *9*, 818−832.
(8) Stoeckli, M.; Staab, D.; Staufenbiel, M.; Wiederhold, K. H.; Signor, L. *Anal. Biochem.* **2002**, *311*, 33−39.
(9) Reyzer, M. L.; Caprioli, R. M. *Curr. Opin. Chem. Biol.* **2007**, *11*, 29−35.
(10) Svatos, A. *Anal. Chem.* **2011**, *83*, 5037−5044.
(11) Colliver, T. L.; Brummel, C. L.; Pacholski, M. L.; Swanek, F. D.; Ewing, A. G.; Winograd, N. *Anal. Chem.* **1997**, *69*, 2225−2231.
(12) Ostrowski, S. G.; Van Bell, C. T.; Winograd, N.; Ewing, A. G. *Science* **2004**, *305*, 71−73.
(13) Fletcher, J. S. *Analyst* **2009**, *134*, 2204−2215.
(14) Szakal, C.; Narayan, K.; Fu, J.; Lefman, J.; Subramaniam, S. *Anal. Chem.* **2011**, *83*, 1207−1213.
(15) Altelaar, A. F. M.; Klinkert, I.; Jalink, K.; de Lange, R. P. J.; Adan, R. A. H.; Heeren, R. M. A.; Piersma, S. R. *Anal. Chem.* **2005**, *78*, 734−742.
(16) Piehowski, P. D.; Carado, A. J.; Kurczy, M. E.; Ostrowski, S. G.; Heien, M. L.; Winograd, N.; Ewing, A. G. *Anal. Chem.* **2008**, *80*, 8662−8667.
(17) Carado, A.; Kozole, J.; Passarelli, M.; Winograd, N.; Loboda, A.; Wingate, J. *Appl. Surf. Sci.* **2008**, *255*, 1610−1613.
(18) Miura, D.; Fujimura, Y.; Yamato, M.; Hyodo, F.; Utsumi, H.; Tachibana, H.; Wariishi, H. *Anal. Chem.* **2010**, *82*, 9789−9796.
(19) Zimmerman, T. A.; Rubakhin, S. S.; Romanova, E. V.; Tucker, K. R.; Sweedler, J. V. *Anal. Chem.* **2009**, *81*, 9402−9409.
(20) Zimmerman, T. A.; Rubakhin, S. S.; Sweedler, J. V. *J. Am. Soc. Mass Spectrom.* **2011**, *22*, 828−836.
(21) Holscher, D.; Shroff, R.; Knop, K.; Gottschaldt, M.; Crecelius, A.; Schneider, B.; Heckel, D. G.; Schubert, U. S.; Svatos, A. *Plant J.* **2009**, *60*, 907−918.
(22) Fletcher, J. S.; Rabbani, S.; Henderson, A.; Lockyer, N. P.; Vickerman, J. C. *Rapid Commun. Mass Spectrom.* **2011**, *25*, 925−932.
(23) Römpp, A.; Guenther, S.; Schober, Y.; Schulz, O.; Takats, Z.; Kummer, W.; Spengler, B. *Angew. Chem., Int. Ed.* **2010**, *49*, 3834−3838.
(24) Römpp, A.; Guenther, S.; Takats, Z.; Spengler, B. *Anal. Bioanal. Chem.* **2011**, *401*, 65−73.
(25) Guenther, S.; Römpp, A.; Kummer, W.; Spengler, B. *Int. J. Mass Spectrom.* **2011**, *305*, 228−237.
(26) Invitrogen product information DiOC6(3), http://products.invitrogen.com/ivgn/product/D273 (accessed December 15, 2011).
(27) Bouschen, W.; Schulz, O.; Eikel, D.; Spengler, B. *Rapid Commun. Mass Spectrom.* **2010**, *24*, 355−364.
(28) Koestler, M.; Kirsch, D.; Hester, A.; Leisner, A.; Guenther, S.; Spengler, B. *Rapid Commun. Mass Spectrom.* **2008**, *22*, 3275−3285.
(29) Guenther, S.; Koestler, M.; Schulz, O.; Spengler, B. *Int. J. Mass Spectrom.* **2010**, *294*, 7−15.
(30) Stryer, L. *Biochemistry*, 4th ed.; W. H. Freeman and Company: New York, 1995.
(31) Korchak, H. M.; Rich, A. M.; Wilkenfeld, C.; Rutherford, L. E.; Weissmann, G. *Biochem. Biophys. Res. Commun.* **1982**, *108*, 1495−1501.
(32) The LIPID MAPS−Nature Lipidomics Gateway, http://www.lipidmaps.org/ (accessed December 6, 2011).
(33) METLIN: Metabolite and Tandem MS Database, http://metlin.scripps.edu/ (accessed November 16, 2011).
(34) Vazquez-Boland, J. A.; Kuhn, M.; Berche, P.; Chakraborty, T.; Dominguez-Bernal, G.; Goebel, W.; Gonzalez-Zorn, B.; Wehland, J.; Kreft, J. *Clin. Microbiol. Rev.* **2001**, *14*, 584.